International Journal of Engineering Research & Technology (IJERT)
ISSN: 2278-0181
Vol. 4 Issue 12, December-2015

De-Noising with Spline Wavelets and SWT

Tilak T. N. * and Krishnakumar S.
School of Technology & Applied Sciences
Mahatma Gandhi University
Edappally, Kochi-24, India

***Abstract*— This paper explores the difference in performance of spline wavelets of the bi-orthogonal type in de-noising images corrupted by Additive White Gaussian Noise. The dependence of the peak signal-to-noise ratio and the mean squared error on the filter characteristics of the wavelets, when stationary wavelet transform is used in the de-noising process, is investigated. It is found that the de-noising action augments with use of wavelet of lower effective length for its high pass reconstruction filter. For wavelets with equal effective lengths for their high pass reconstruction filters, a relation similar to the above, exists for the high pass decomposition filters. 'Bior1.1' (bi-orthogonal spline wavelet 1.1) is found to be the most suitable wavelet in the family, for de-noising. 'Bior 3.1' is found to be an odd member in the family and is not at all suitable for de-noising, the reason for which is traced to the lack of smoothness of its decomposition scaling function.**

Keywords*— *Spline wavelet, stationary wavelet transform, additive white gaussian noise, thresholding.

I. INTRODUCTION

The Fourier Transform has been the dominant tool for image processing, in the frequency domain. But the Wavelet Transform has emerged as an even better instrument for the purpose. There are several factors which contribute to superiority of the Wavelet Transform over the Fourier transform, in image processing applications.

The Fourier Transform has a sinusoidal basis function which extends from $-\infty$ to $+\infty$. It makes use of only the sine and cosine functions [1]. With Fourier Transform we compare the signal to be analyzed, in terms of sinusoidal functions of different frequencies. Therefore it provides good frequency resolution, but then, the resolution in time is zero. This is actually a manifestation of Heisenberg's uncertainty principle which holds that a signal can be said to occupy some position inside a rectangle of dimension $\Delta t \times \Delta\omega$ within the time-frequency space but the exact position inside this rectangle cannot be determined [2]. However, a solution to circumvent this problem is provided by what is called "Multi- Resolution Analysis" (MRA). MRA means analysis of the image or signal at different resolutions. In MRA, the details of the image at a particular resolution, say r_k, is estimated as the difference of information of its approximations at the resolutions r_k and r_{k-1}, $k \in Z$, where the resolutions r_{k-1} and r_k follow an ascending order [3]. The Wavelet Transform helps to make MRA realizable. It can break up input data in to different frequency parts and then analyze each of these parts with a resolution suited for the scale of that part [4]. This means that small details as well as coarse details in an image can be perceived. In Wavelet Transform, shifted and translated versions of a prototype wavelet constitute a set of orthogonal basis functions. Wavelets are little wave-like functions which can be represented as:

$$f_{s,t}(u) = |s|^{-½} f\left(\frac{u-t}{s}\right) \quad s,t \in R,\ s \neq 0, \qquad (1)$$

and produced by dilations and translations of the function ' f ' [5]. An appropriate combination of wavelets can be used to represent any signal [6]. The original wavelet before stretching or shrinking is called "Mother wavelet". Wavelets are extremely adaptable for analyzing any signal; this is consequent of their ability to be dilated and translated. Translation of the wavelet determines the location to analyze, and scale changes of the wavelet helps to analyze the signal at different frequencies [2].

A wavelet function $\Psi \in L^2(R)$ has a varying frequency. The function is 0 except for a short duration in time. Therefore a wavelet is said to have a "compact support". This property enables to achieve perfect reconstruction [7]. A wavelet should also comply with the following three conditions [2]:

(i) 0 mean value, i.e.,

$$\int_{-\infty}^{+\infty} \Psi \, dt = 0 \qquad (2)$$

,

(ii) Ψ is normalized, i.e.,

$$\|\Psi\|^2 dt = 1 \qquad (3)$$

and

(iii) the admissibility condition represented as:

$$\int_{-\infty}^{+\infty} \frac{|\Psi(\omega)^2|}{|\omega|} d\omega < \infty, \qquad (4)$$

where $\Psi(\omega)$ is the Fourier Transform of Ψ.

This paper investigates the de-noising performance of bi-orthogonal spline wavelets using StationaryWavelet Transform (SWT).

II. MATERIALS AND METHODS

A. *Bi-orthogonal wavelets*

First, By the term 'bi-orthogonal', we mean two functions or 'bases' which are mutually orthogonal, but each of which need not form an orthogonal set. For bi-orthogonal wavelets, we use two different scaling functions and two different wavelet functions. One set of scaling and wavelet functions (Φ and Ψ) is used in the decomposition step and the other set (Ψ and $\widehat{\Psi}$) is used in the reconstruction step. This provides interesting features that are not possible by using one and the same filters for decomposition and reconstruction as what we do in the orthogonal case. Also, filter banks comprising bi-

orthogonal filters are more flexible and can be designed easily. Bi-orthogonal wavelets have linear phase which is good for reconstruction of images [8]. In this study we make use of the bi-orthogonal spline wavelets listed as: 'bior 1.1', 'bior 1.3', 'bior 1.5', 'bior 2.2', 'bior 2.4', 'bior 2.6', 'bior 2.8', 'bior 3.1', 'bior 3.3', 'bior 3.5', 'bior 3.7', 'bior 3.9', 'bior 4.4', 'bior 5.5' and 'bior 6.8'

B. Corruption of image by adding noise

For studying the de-noising performance, first of all we create a noisy image by adding noise of desired type and variance to the selected original image. Additive White Gaussian Noise (AWGN) is chosen for corrupting the original image because most of the noisy digital images contain this type of noise [9]. Additive Gaussian Noise can be represented by the noise model: i (x, y) = t(x, y) + r(x, y), where i(x, y) is the pixel in the corrupted image, t(x, y) is the true pixel value and r(x, y) represents the random Gaussian distributed noise [10]. We have used an AWGN of variance $\sigma^2 = 0.07$ to corrupt the image. The noise variance value 0.07 is in a 0 — 1 scale. Such a high value for the added noise is selected to enable good visual comparison between the noisy image and the de-noised images.

C. Stationary wavelet transform

Image de-noising process using a wavelet transform called Discrete Wavelet Transform (DWT) uses the pyramidal algorithm proposed by Stephen Mallat. But DWT has the drawback that it is not shift-invariant. This amounts to that the transform of a time-shifted version of an image differs from that of the original image. This is a consequence of the decimation associated with DWT. Lack of shift-invariance results in production of artifacts in the reconstructed image. The Stationary Wavelet Transform (SWT) is a shift-invariant transform. It has better de-noising performance than DWT [11]. An algorithm which implements SWT is the 'a´ trous' algorithm. However, SWT involves additional computation and is basically redundant [12]. But the benefits offered by SWT outweigh its shortcomings. Hence we have adopted SWT in this work.

D. Levels of decomposition

The decomposition using SWT can be continued until only 1 sample is left. In practice the number of levels of decomposition is determined by factors such as the noise content and quality of the reconstructed image. We have used the lena image (jpeg) of size 512 × 512 for the study. 'J' levels of decomposition, J ε Z, are possible with SWT so far as the size of the image is divisible by 2^J. But more than 3 levels of decomposition result in blurring the image. It is the consequence of removal of more information from the image on account of thresholding at the higher levels. Hence in this work we have used an optimum 3 levels of decomposition for analysis with each wavelet.

E. Thresholding

We adopt soft thresholding in this work. In soft thresholding the threshold value is subtracted from all coefficients whose values are larger than it and the remaining coefficients are thrown away [13]. Here, unlike hard thresholding, abrupt discontinuities are not produced. This has prompted us to use soft thresholding.

F. Performance measures

De-noising performance evaluation is carried out using two performance measures namely, Mean Squared Error (MSE) and Peak Signal to Noise Ratio (PSNR) of the de-noised images. These are defined as:

$$MSE= \frac{1}{m\,n}\sum_{i=1}^{m}\sum_{j=1}^{n}(X(i,j)-X'(i,j))^2 \quad (5)$$

$$PSNR =10\log\left(\frac{255^2}{MSE}\right)dB \quad (6)$$

where X is the original (noise-less) image, X' is the de-noised image, X(i, j) is the pixel value at the i^{th} row and j^{th} column of the digital image and m and n are the number of rows and columns [14].

The MSE and PSNR are calculated for the de-noised images resulting from de-noising using each wavelet.

The visual quality of the de-noised images is also examined. There is no generally accepted objective method for assessing visual quality of de-noised images. However two criteria in use are absence of artifacts and preservation of edges in the original image.[15].

III. RESULTS AND DISCUSSION

The noisy image is shown in Fig. 1. Fig. 2 and Fig. 3 show the de-noised images with the obtained maximum and minimum values of PSNR, respectively. The MSE and PSNR corresponding to de-noising with the different bi-orthogonal wavelets are shown in Table 1.

The decomposition process using SWT involves convolution of the image matrix with a low pass filter and a high pass filter. These filters are respectively labeled as LoD and HiD and the values of their effective lengths are given in columns 4 and 5 respectively in Table 1. Similarly the reconstruction process involves convolution of the image matrix with another set of filters containing a low pass filter and a high pass filter indicated as LoR and HiR. The values of the effective lengths of these filters are given in columns 6 and 7 respectively in Table 1. Usually the high frequency components in an image comprise the noise in the image.

Fig.1. Noisy image

Fig.2 . Image de-noised with 'bior 1.1'

Fig.3. Image de-noised with 'bior 3.1'

Therefore it is reasonable for us to examine the features of HiD and HiR to relate the same to the variations in the de-noising performance of the different wavelets used for the study. The output of low pass filter contains approximation of the image.

It is observed that the estimated values of the PSNR (and MSE) vary with the different wavelets used in the SWT for the de-noising process. From Table 1 it can be seen that the variations in the PSNR values have some amount of relationship with the effective lengths of HiR and HiD. A detailed inspection of the corresponding values leads to the following observations:

1. The PSNR decreases with increase in the effective length of HiR. This fact is observed to be true in all the de-noising cases under consideration, except in the cases of de-noising with 'bior 3.1', 'bior 3.3' and 'bior 3.5'. 'Bior 3.1' gives the lowest PSNR (34.5294) even though this wavelet has a low value 4 for effective length of HiR. In fact, 'bior 3.1' has the second lowest effective length of HiR when we consider the corresponding values of all the other members in the bi-orthogonal spline wavelet family. Thus 'bior 3.1' is found to have an odd behavior, the reasons for which shall be explored

TABLE 1

PSNR, MSE and effective filter lengths of the wavelets						
Wavelet	*MSE*	*PSNR dB*	*Effective length of filters*			
			LoD	*HiD*	*LoR*	*HiR*
bior 1.1	12.4334	37.1849	2	2	2	2
bior 1.3	13.0208	36.9844	6	2	2	6
bior 1.5	13.2655	36.9036	10	2	2	10
bior 2.2	13.0943	36.9600	5	3	3	5
bior 2.4	13.2460	36.9100	9	3	3	9
bior 2.6	13.3893	36.8632	13	3	3	13
bior 2.8	13.5105	36.8241	17	3	3	17
bior 3.1	22.9163	34.5294	4	4	4	4
bior 3.3	13.6426	36.7818	8	4	4	8
bior 3.5	13.4364	36.8480	12	4	4	12
bior 3.7	13.5213	36.8206	16	4	4	16
bior 3.9	13.6092	36.7925	20	4	4	20
bior 4.4	13.4691	36.8374	9	7	7	9
bior 5.5	13.6570	36.7773	9	11	11	9
bior 6.8	13.8360	36.7207	17	11	11	17

later. Hence the following discussion skips 'bior 3.1', for the time being. As we move from 'bior 2.8' to 'bior 3.3', the PSNR decreases even though the effective length of HiR has decreased. The reason for this is an increase in the actual values of HiR represented by the increased value of HiR_{max} (maximum value of HiR) given in Table 2. Due to this increase in values of HiR, high amplitude coefficients containing noise are retained. An effect just opposite to this is observed in the case of 'bior 3.5'.

'Bior 1.1' gives the maximum value of PSNR which is 37.1849. Also, the effective length of HiR has the lowest value for 'bior 1.1'. This fact agrees with our above observation regarding relation between PSNR and effective length of HiR.

Large effective length of HiR means large number of non-zero filter points in the filter. Since this high pass filter with the large number of non-zero coefficients is convolved with the coefficients resulting from decomposition of the noisy digital image which have subsequently been thresholded, such a convolution gives rise to high frequency components spread over a large extent and carries the noise components that have not been removed in the thresholding process. This explains the reduction in PSNR with increase in effective length of HiR.

2. When the effective lengths of HiR for two different wavelets are equal, the PSNR is found to decrease with increase in the effective length of HiD. This is evident by observing the PSNR values of the set of wavelets comprising 'bior 2.4', 'bior 4.4' and 'bior 5.5', each of which has an effective length 9 for HiR. The PSNR values obtained on de-noising with these wavelets decrease regularly as the effective lengths of HiD increase. This is shown separately in Table 3 for easy reference.

An identical effect is noticed on observing the de-noising performance of 'bior 2.8' and 'bior 6.8'. Both of these wavelets have effective length 17 for HiR. The PSNR is found to have decreased as the effective length of HiD has increased

3. The influence of effective length of HiD on de-noising performance is considerably less than that of HiR. This can be established in the following way. We have already established above that (i) the PSNR decreases with increase in the effective length of HiR and that (ii) when the effective lengths of HiR of 2 bi-orthogonal spline wavelets are equal, the PSNR decreases with increase in the effective length of HiD.

As we move from 'bior 1.5' to 'bior 2.2' the effective length of HiD increases from 2 to 3, effective length of HiR decreases from 10 to 5 and PSNR increases. Also when we move from 'bior 3.9' to 'bior 4.4', the effective length of HiD undergoes an increase from 4 to 7; at the same time, effective length of HiR decreases from 20 to 9 and the PSNR value increases. Here the effective length of HiD has increased by 1 point in the former case and by 3 points in the latter case. On the other hand, the effective lengths of HiR in these cases have had decrease and that by considerably larger numbers of points. In both the instances the PSNRs have only increased; this increase in PSNR is in tune with our observation 1, i.e., the increase in PSNR accompanies the decrease in effective length of HiR. In this context it may be noted that the aforesaid increases in effective lengths of HiD have had no noticeable effect on the PSNR. This establishes that effective length of HiD has considerably lesser influence on de-noising performance, compared to effective length of HiR; also this influence is in tune with observation No. 2 above.

Table 2. Maximum values of HiR for 'bior 2.8','bior 3.3' and 'bior3.5'.

Wavelet	HiR_{max}
bior 2.8	0.4626
bior 3.3	0.9944
bior 3.5	0.9667

TABLE 3.

PSNR and effective lengths of HiD for wavelets with HiR of effective length 9.

Wavelet	Effective length of HiD	PSNR dB
bior 2.4	3	36.9100
bior 4.4	7	36.8374
bior 5.5	11	36.7773

The apparent dominance of the dependence of effective length of HiR on PSNR, compared to that of HiD, is consequent of the larger value of effective length of HiR compared to that of HiD, or in other words, due to the larger numbers of non-zero filter points of HiR when compared to those of HiD; it can be seen that in most cases, the effective length of HiR is 2 to 4 times that of HiD.

Now, we may investigate the reason for the odd behavior of 'bior 3.1'.

The decomposition scaling function of 'bior 3.1' is shown in Figure 4. As what can be seen from Figure 4, this function is not at all a smooth one. It is scaling function bases that generate the wavelet basis functions [2]. Hence the decomposition wavelet function of 'bior 3.1' is also not smooth. The basic two-scale relation in MRA is:

$$\Phi(t) = \sum_k p(k)\, \Phi(2t - k), \quad k \varepsilon Z, \quad (7)$$

where $\Phi(t)$ is the scaling function and $p(k)$ is the discrete sequence of coefficients resulting from the decomposition. This

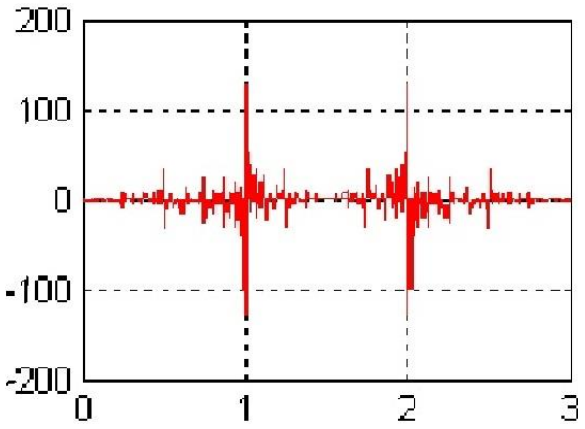

Fig. 4. Decomposition scaling function of 'bior 3.1'

equation indicates that the scaling function at a particular resolution can be decomposed in to a linear combination of scaling functions at the next higher resolution [2]. The discrete sequence p(k) of the coefficients resulting from the decomposition constitutes the low pass filter in the wavelet decomposition. Since the decomposition scaling function is not smooth, its regularity is poor and the decomposition low pass filter has a high variance. This is also evident from Table 4

TABLE 4.

Variances of the effective lengths of LoD	
Wavelet	Var (LoD)
bior1.1	0
bior1.3	0.1396
bior1.5	0.0956
bior2.2	0.2208
bior2.4	0.1350
bior2.6	0.0983
bior2.8	0.0777
bior3.1	0.6667
bior3.3	0.2662
bior3.5	0.1696
bior3.7	0.1255
bior3.9	0.1001
bior4.4	0.0934
bior5.5	0.0567
bior6.8	0.0565

which shows the variances of LoD (Var (LoD)) of the different wavelets. It can be seen that 'bior 3.1' has the highest value for "variance" or "dispersion" of LoD. This explains the reason for the odd behavior and the poor de-noising performance of 'bior 3.1'. Also the visual quality of the de-noised images is found to have changes following the changes in the PSNR values.

IV. CONCLUSIONS

This paper explores de-noising performance of the different bi-orthogonal spline wavelets, when SWT is used as the transform for the de-noising operation. The de-noising action is found to improve with the use of bi-orthogonal wavelet of lower effective length for its high pass reconstruction filter. When the effective lengths of high pass reconstruction filter for any two bi-orthogonal spline wavelets are equal, the PSNR decreases with increase in the effective length of high pass decomposition filter. The influence of effective length of high pass decomposition filter on de-noising performance is considerably less than that of high pass reconstruction filter; this is due to the fact that the latter has larger number of non-zero filter points than the former.

The maximum value of PSNR is obtained by de-noising with the bi-orthogonal spline wavelet with the minimum effective reconstruction filter length which is 'bior 1.1'. 'Bior 1.1' is hence the most suitable bi-orthogonal spline wavelet for de-noising images corrupted by AWGN. 'Bior 3.1' is found to be an odd member in the bi-orthogonal spline wavelet family. This wavelet gives the lowest PSNR. Therefore 'bior 3.1' is not at all suitable for de-noising. The odd behavior and the worst de-noising performance of 'bior3.1' are traced to be consequent of the lack of smoothness of its decomposition scaling function. It is also found that the visual quality of the images resulting from de-noising using the different bi-orthogonal spline wavelets follow the changes in the PSNR values obtained.

REFERENCES

[1] I.W. Selesnick, R.G. Baraniuk, N.G. Kingsbury, "The dual-tree complex wavelet transform". IEEE Sigl. Proc. Mag. 2005; 22: 123 ─ 151.
[2] Y. Sheng, The Transforms and Applications Handbook, 2 nd ed., Boca Raton, FL, USA, CRC Press, 2000.
[3] S.G.Mallat, "A theory for multi-resolution signal decomposition: the wavelet representation", IEEE Trans. Patt. An. & Mac. Int., 1989; 11: 674 ─ 693.
[4] I. Daubechies, Ten Lectures On Wavelets. Philadelphia, PA 19104 ─ 2688 USA; SIAM, 1992.
[5] I. Daubechies, "Orthonormal bases of compactly supported wavelets", J Com. Pure App. Math., 1988, XLI: 909 ─ 996.
[6] G. Strang, "Wavelets", Am. Sci. J, 1994, 82: 250 ─ 255.
[7] M. Vetterli, C. Herley, "Wavelets and filter banks: theory and design", IEEE Trans. SigL. Proc. 1992, 40: 2207 ─ 2232.
[8] Krishnakumar, Basantkumar, R.Shah, "Analysis of efficient wavelet based volumetric image compression", Int. J Im. Proc., 2012, 6: 113 ─ 122.
[9] M. Chui, Y Feng, W.Wang, Z. Li, X. Xu, "Image de-noising method with adaptive bayes threshold in nonsubsampled contourlet domain", 2012 AASRI Conf.on Comp. Intelligence and Bioinformatics, 1 ─ 2 July 2012; Changsha, China: ELSEVIER. pp. 512 ─ 518.
[10] S.D. Ruikar, D.D. Doye, "Wavelet based image de-noising technique",. Int. J Adv. Comp., Sc. & App., 2011, 2: 49 ─ 53.

[11] J.Starck, J.Fadili, F. Murtagh, "The undecimated wavelet decomposition and its reconstruction", IEEE Trans. Im. Proc., 2007, 16: 297 ─ 309.
[12] M.G.Audicana, X.Otazu, O.Fors, A.Seco, "Comparison between Mallat's and the 'a` trous' discrete wavelet transform based algorithms for the fusion of multispectral and panchromatic images", Int. J Rem. Sens., 2005, 000: 1 ─ 19.
[13] L.Sendur, I.W. Selesnick, "Bivariate shrinkage functions for wavelet-based de-noising exploiting interscale dependency", IEEE Trans. Sigl Proc., 2002, 50: 2744 ─ 2756.
[14] S. Priyadharshini, K. Gayathri, S. Priyanka, K. Eswari, "Image de-noising based on adaptive wavelet multiscale thresholding method", Int. J Sci. & Mod. Eng., 2013, 1: 37 ─ 39.
[15] F. Luisier, T. Blu, M. Unser, "A new SURE approach to image de-noising: interscale orthonormal wavelet thresholding", IEEE Trans. Im. Proc., vol.16, No.3, March 2007.